

# Three-body mechanism of $\eta$ production

K. P. Khemchandani<sup>1</sup>, N. G. Kelkar<sup>2</sup> and B. K. Jain<sup>3</sup>

<sup>1</sup>*Nuclear Physics Division, Bhabha Atomic Research Centre, Mumbai  
400085, India*

<sup>2</sup>*Departamento de Fisica, Universidad de los Andes, Cra. 1E, No. 18A-10,  
Santafe de Bogota, Colombia*

<sup>3</sup>*Physics Department, University of Mumbai, Mumbai - 400098, India,  
Saha Institute of Nuclear Physics, 1/AF, Bidhan Nagar, Kolkatta, India*

## Abstract

The usefulness of the three-body mechanism of  $\eta$ -meson production is tested by extending to high energies a recently developed two step model of the  $pd \rightarrow {}^3\text{He} \eta$  reaction by us, which was successful in reproducing the energy dependence of the data near threshold. The  $\eta$  production in this model, proceeds in two steps via the  $pp \rightarrow \pi d$  and  $\pi N \rightarrow \eta p$  reactions with the intermediate particles being off-shell. The final state interaction(FSI) is incorporated through a  $T$ -matrix for  $\eta {}^3\text{He}$  elastic scattering constructed using few body equations. In a comparison of the calculated angular distributions with some recently available data, we discover the limitations of the model at high energies.

PACS numbers: 13.75.-n, 25.40.Ve, 25.10.+s

*Keywords:*  $\eta$ -meson production, reaction mechanism, two-step model

# 1 Introduction

The importance of the three-body mechanism (3-bm) in meson production was first shown in [1, 2] by Laget and Lecolley. Whereas in the pion producing reactions  $pd \rightarrow {}^3\text{H} \pi^+$  and  $pd \rightarrow {}^3\text{He} \pi^0$ , this mechanism accounted for the discrepancies left out at backward angles by the one- and two-body mechanisms, in the case of the  $pd \rightarrow {}^3\text{He} \eta$  reaction, it was found to play the dominant role in reproducing the Saturne data at threshold [3] and that at high energies [4] for  $\theta_\eta = 180^\circ$ . The one- and two-body mechanisms in the  $pd \rightarrow {}^3\text{He} \eta$  reaction, were found to underestimate the experimental cross sections by two orders of magnitude. Motivated by these works, more recently, two step models [5, 6, 7] which essentially involved the 3-bm, were constructed to study the  $pd \rightarrow {}^3\text{He} \eta$  data near threshold [3, 8]. The  $\eta$ -meson in these models is produced in two steps via the  $pp \rightarrow \pi d$  and  $\pi N \rightarrow \eta N$  reactions, thus involving the participation and sharing of momentum by three nucleons which is typical of a 3-bm (see Fig. 1). The calculation in [7] is the most involved one available on the  $pd \rightarrow {}^3\text{He} \eta$  reaction in literature. In it, (i) the final state  $\eta$ - ${}^3\text{He}$  interaction which is crucial for the energy dependence of this reaction is incorporated through a T-matrix constructed using few-body equations and (ii) the fermi motion and off-shell nature of the intermediate particles in the 3-bm is taken into account properly. Some other theoretical investigations of the  $pd \rightarrow {}^3\text{He} \eta$  reaction at threshold and high energies can also be found in [9, 10]. The work in [10] needs a special comment to which we shall return later.

The explanation for the dominance of the 3-bm in  $\eta$  production is straightforward. Due to the large mass of the  $\eta$ -meson ( $\sim 547$  MeV), the momentum transfer involved in this reaction is as large as 900 MeV/c near threshold. The 3-bm allows this large momentum to be shared among three nucleons, thus making it easily digestible by the nucleus than in the one- and two-body mechanisms where the nuclear form factor (evaluated at large momenta) is rather small. Since the two step model alone could reproduce the strong energy dependence of the threshold data [7] and given the fact that the momentum transfer in the  $pd \rightarrow {}^3\text{He} \eta$  reaction continues to be large ( $\sim 650$  MeV/c) even at 1 GeV above threshold, one would speculate that the same model would also be successful in reproducing the recently reported angular distributions [11] at high energies. An extension of the model in [7] to compare with the high energy data of [11], therefore, seems timely.

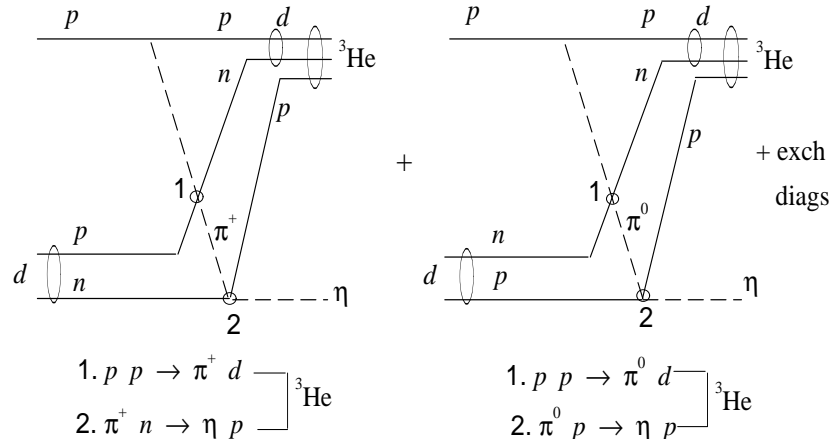


Figure 1: The diagram corresponding to the three-body mechanism of  $\eta$ -meson production in the  $pd \rightarrow {}^3\text{He} \eta$  reaction.

However, before proceeding further, let us recapitulate the following observations from the different 3-bm calculations carried out in the literature at energies beyond threshold: (a) the success of the 3-bm reported in [2] for the the  $pd \rightarrow {}^3\text{He} \eta$  reaction over a range of proton beam energies up to 2.5 GeV, was confined to one particular angle, namely,  $\theta_\eta = 180^\circ$ , (b) in case of pion production at high energies, the 3-bm was mostly responsible in removing the discrepancies between theory [1] and data at backward pion angles, (c) the theoretical estimates [6, 12] of angular distributions (at threshold and at high energies) of the  $pd \rightarrow {}^3\text{H} K^+$  reactions made within a two step model, seem to indicate backward peaked cross sections and (d) the cross sections calculated in [7] for the  $pd \rightarrow {}^3\text{He} \eta$  reaction within the two step model were nearly isotropic near threshold; however, there was a hint of a backward peak as one moved about 10 MeV away from threshold.

That is, in all, the existing 3-bm calculations point toward a backward angle dominance of the cross sections in this model. In contrast to this, the measured angular distributions of the  $pd \rightarrow {}^3\text{He} \eta$  reaction from about 90-200 MeV above threshold are all forward peaked [11, 13]. Thus, a priori, one would doubt the possibility of the two-step model being able to reproduce the high energy data. Indeed in [14], in an attempt to reproduce the differential cross section data at beam energies of 930, 965, 1037 and 1100

MeV, using a Monte-Carlo description of the  $pd \rightarrow {}^3\text{He} \eta$  reaction within a two-step model, the authors find backward peaked cross sections which are in complete disagreement with data, but are however, in line with the above theoretical findings. A very recent work [10], which reports the success of the two step model in reproducing the data on angular distributions mentioned above, is then isolated in its findings. The results in [10] have been obtained using a factorization approximation, which neglects the off-shell nature of the intermediate pion propagator as well as the t-matrices for the  $\pi N \rightarrow \eta N$  and  $pp \rightarrow \pi^+ d$  reactions. It restricts the pion in an ad hoc way to go at  $0^\circ$ . Besides, though not mentioned clearly, it seems that the final state interaction has also been incorporated within a factorization approximation as in [5]. The model with such approximations, does not truly represent the three-body Feynman diagram of Fig. 1 (where the intermediate particles are off-shell), hence the results of such specious models should be treated with caution. To obtain a proper estimate of the contribution of the 3-bm at higher energies, we extend our earlier calculation [7] to evaluate the differential cross sections at 930, 965, 980, 1037 and 1100 MeV beam energy for which data are available. These calculations include the off-shell and final state interaction effects elaborately and do not restrict the pion to any specific angle. Unlike [10] and as expected, partly from our earlier work [7] and partly from calculations of other reactions with 3-bm in literature (mentioned in (c) above), we get backward peaked angular distributions which are at variance with the corresponding forward peaked data. The cause for this discrepancy may lie in the interaction among the particles in the intermediate state or the increasing importance of some other mechanisms which need to be investigated. We therefore conclude that the 3-bm calculations of the  $pd \rightarrow {}^3\text{He} \eta$  reaction at energies away from the threshold do not reproduce the observed forward peaking of the  $\eta$  angular distribution seen in the Uppsala data. This is in contradiction with the observations reported in [10].

In the next section we describe the inputs of the model only briefly and move on to the discussion of the results. The details of the model can be found in [7].

## 2 Two step model of the $pd \rightarrow {}^3\text{He} \eta$ reaction

In the two step model of  $\eta$  production, the incident proton interacts with one of the nucleons in the deuteron ( $d$ ) to produce a deuteron ( $d'$ ) and pion, which in turn interacts with the other nucleon in  $d$  to produce an  $\eta$ -meson and a proton. This proton and the  $d'$  combine to form the  ${}^3\text{He}$  nucleus. The transition matrix for the  $pd \rightarrow {}^3\text{He} \eta$  reaction which includes the final state  $\eta$ - ${}^3\text{He}$  interaction is given as,

$$T = \langle \vec{k}_\eta; m_3 | T_{pd \rightarrow {}^3\text{He} \eta} | \vec{k}_p; m_1 m_2 \rangle + \sum_{m'_3} \int \frac{d\vec{q}}{(2\pi)^3} \frac{\langle \vec{k}_\eta; m_3 | T_{\eta {}^3\text{He}} | \vec{q}; m'_3 \rangle}{E(k_\eta) - E(q) + i\epsilon} \langle \vec{q}; m'_3 | T_{pd \rightarrow {}^3\text{He} \eta} | \vec{k}_p; m_1 m_2 \rangle. \quad (1)$$

The matrix elements  $\langle | T_{pd \rightarrow {}^3\text{He} \eta} | \rangle$  in the above equation correspond to the Born amplitude for the  $pd \rightarrow {}^3\text{He} \eta$  reaction.  $\vec{k}_p$  and  $\vec{k}_\eta$  are the asymptotic momenta of the particles in the initial and final states and  $m_1$ ,  $m_2$  and  $m_3$  are the spin projections of the proton, deuteron and  ${}^3\text{He}$  respectively. The  $T$ -matrix for  $\eta$ - ${}^3\text{He}$  elastic scattering,  $T_{\eta {}^3\text{He}}$ , is evaluated using four-body equations for the  $\eta(3N)$  system. The Born amplitude is given within the two step model as,

$$\begin{aligned} \langle | T_{pd \rightarrow {}^3\text{He} \eta} | \rangle = & i \int \frac{d\vec{p}_1}{(2\pi)^3} \frac{d\vec{p}_2}{(2\pi)^3} \sum_{int m'_s} \langle pn | d \rangle \langle \pi d | T_{pp \rightarrow \pi d} | pp \rangle \quad (2) \\ & \times \frac{1}{(k_\pi^2 - m_\pi^2 + i\epsilon)} \langle \eta p | T_{\pi N \rightarrow \eta p} | \pi N \rangle \langle {}^3\text{He} | pd \rangle, \end{aligned}$$

where the sum runs over the spin projections of the intermediate off-shell particles. The four momentum of the intermediate pion,  $k_\pi$ , which could either be a  $\pi^+$  or  $\pi^0$  is given as,

$$\begin{aligned} \vec{k}_\pi &= \frac{\vec{k}_p}{2} + \frac{2}{3}\vec{k}_\eta + \vec{p}_1 + \vec{p}_2 \quad (3) \\ k_\pi^0 &= E_\eta + \frac{1}{3}E_{{}^3\text{He}} - \frac{1}{2}E_d, \end{aligned}$$

where  $\vec{p}_1$  and  $\vec{p}_2$  are the fermi momenta of the intermediate nucleons. Each of the individual matrix elements in the above equation is expressed in terms of partial wave expansions. The matrix elements for the  $pp \rightarrow \pi d$  reaction,

parametrized in terms of the available experimental data are taken from Ref. [15]. For the  $\pi N \rightarrow \eta p$  reaction, we use the single resonance, coupled channel model of Ref. [16]. This model treats the  $\pi N$ ,  $\eta N$  and  $\pi\pi N$  as coupled channels. We use the  $T$ -matrix in this model with the inclusion of the  $S_{11}$ ,  $P_{11}$  and  $D_{13}$  resonances. Since the  $\eta - P_{11}$  coupling used in Ref. [16], as noticed in [10], does not reproduce the data on  $\pi N \rightarrow \eta N$  reaction, we use it as given in [10]. The matrix elements  $\langle pn|d \rangle$  and  $\langle {}^3\text{He}|pd \rangle$  consist of the deuteron and helium wave functions in momentum space which depend on the momenta  $\vec{p}_1$  and  $\vec{p}_2$  respectively. The details of the wave functions and the  $\eta^3\text{He}$   $T$ -matrix are given in [7]. In the calculation of the  $\eta^3\text{He}$   $T$ -matrix, we use the coupled channel elementary  $t$ -matrix,  $t_{\eta N \rightarrow \eta N}$  as in [17]. This  $t$ -matrix was the one which gave the best agreement in [7] with the threshold data.

### 3 Results and Discussion

Recent measurements of the  $p d \rightarrow {}^3\text{He} \eta$  reaction, from about 22 MeV to 115 MeV above threshold [11, 13] show that, as we go away from the threshold, the angular distribution starts developing anisotropy, which increases with energy. The GEM data [13] show a strong forward peak and the data from the Wasa-Promice collaboration [11] are found to be maximal for  $\cos \theta_\eta \approx +0.5$ . At threshold, the angular distribution is isotropic.

Fig. 2 shows our calculated differential cross sections, using the two step model described in the previous section, along with the experimental data from [11, 13]. The dashed curves represent the plane wave calculations, while the solid lines correspond to the calculations including the  $\eta^3\text{He}$  final state interaction (FSI). We find that the observed trend in the anisotropy of the data is not at all reflected in the calculated results. Unlike the data, the latter peak at backward angles. This in contrast to the findings in [10].

Fig. 3 shows the data and calculation of the spin averaged amplitude which is defined as,

$$|f|^2 = \frac{k_p}{k_\eta} \frac{\sigma_{tot}}{4\pi}, \quad (4)$$

where  $k_p$  and  $k_\eta$  are the proton and  $\eta$  momentum in the center of mass system.  $\sigma_{tot}$  is the angle integrated cross section. In the experiment it is obtained by making a polynomial fit to the data at the available angles

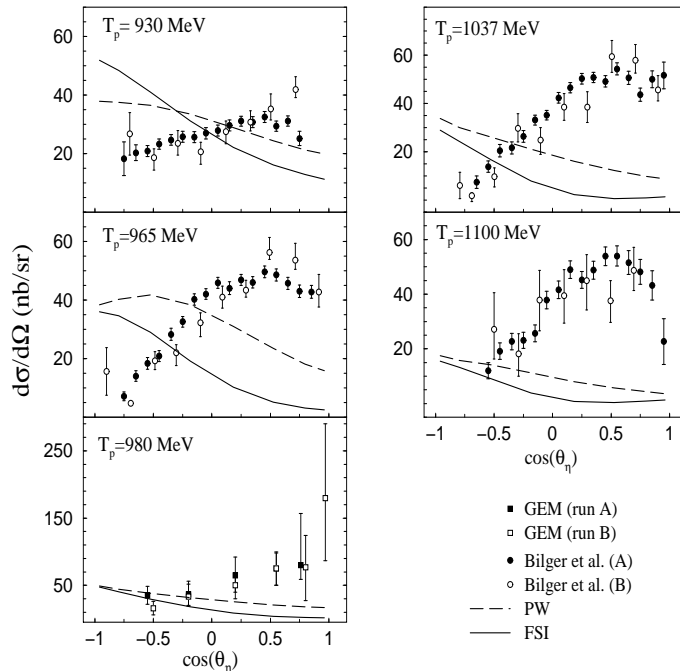


Figure 2: The angular distribution of the  $pd \rightarrow {}^3\text{He}\eta$  reaction. The data are from Ref. [11, 13]. The data points (A) and (B) of [11], represent respectively, the data taken with only the  ${}^3\text{He}$  detected and with  ${}^3\text{He}$  detected in coincidence with two photons. The dashed lines (solid lines) are calculations without (with) inclusion of the final state interaction (FSI).

and then integrating the parameterized distribution. We observe two things: (i) the two step model results are in excellent accord with the data near threshold. The model however underestimates the data at higher energies. (ii) Comparison of the calculated results with and without FSI show that, while near threshold the FSI increases the cross section, at higher energies its effect is to decrease the cross sections. This, as discussed in our earlier work [7], is the reflection of the decreasing importance of the off-shell  $\eta$ - ${}^3\text{He}$  scattering in the final state at high energies.

To see the implication of the restriction on the direction of the intermediate pion, we show in Fig. 4, our calculated results at one beam energy, for pions restricted up to various emission angles. As found in [10], the forward pion emission indeed skews the differential cross section to forward

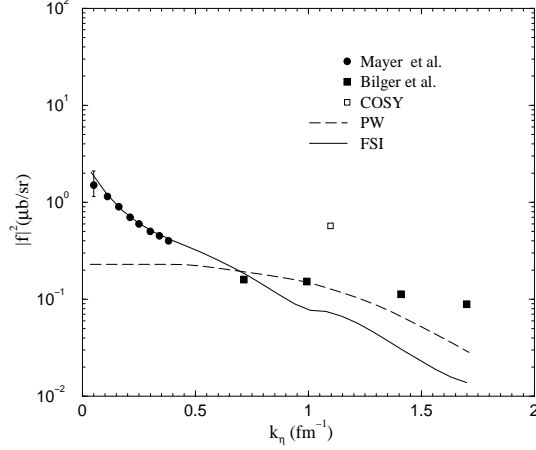


Figure 3: The square of  $pd \rightarrow {}^3\text{He}\eta$  amplitude as defined in eq. (4). The dashed (solid) lines correspond to the calculations without (with) FSI. The data are from refs [8, 11, 13].

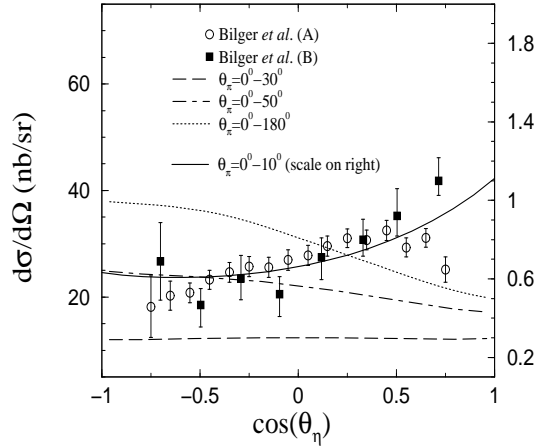


Figure 4: The angular distribution for the  $pd \rightarrow {}^3\text{He}\eta$  reaction at 930 MeV beam energy. The solid line shows the cross section with the intermediate pion angle restricted from 0 to  $10^\circ$  with its scale on the right hand side. The long dashed, dot-dashed and dotted curves show the cross sections obtained after restricting the pion angle from 0 to  $30^\circ$ , 0 to  $50^\circ$  and allowing the full range of 0 to  $180^\circ$  respectively (with the scale given on the left).

angles. As such, this restriction is of course ad hoc. Any legitimacy in this may be sought in the interaction among the particles in the intermediate state. We also see that the cross sections fall with reduction in the range of allowed pion angles. The scale given on the right side of Fig. 4 for the 0 to  $10^0$  restriction (solid line) shows that though the shape of the experimental angular distribution is correctly reproduced, the magnitude is underestimated by about a factor of 40. This is again in contrast to the finding in [10], where the agreement with absolute cross sections, with the pion angle restricted to  $0^0$  is not so bad. The reason for this discrepancy could lie in the neglect of the off-shell effects at the intermediate vertices in the reaction mechanism in [10]. Since we only wish to demonstrate in Fig. 4 the effect of restricting pion angles, these calculations have been done without including the FSI.

## 4 Conclusions

The role of the three-body mechanism had been demonstrated unambiguously in our earlier work on the  $pd \rightarrow {}^3\text{He} \eta$  reaction near threshold [7]. Indeed, isotropic angular distributions and the magnitude of the total cross sections were well reproduced. Extending the model to higher energies (without making any rough approximations outside the spirit of the model) leads to a large discrepancy between model predictions and available data. We believe that any ad hoc manipulations of the model [10], like e.g., restricting the pion to be on-shell and to be produced in the forward direction ( $\theta_{p\pi} = 0$ ), do not represent the three-body mechanism in the context of the Feynman diagram and hence are hard to justify. Had these conditions really been the preferred ones in the three-body mechanism, it should have come out anyway through a proper calculation as performed in the present work. However, this is not the case.

The failure of the model, especially in reproducing data at forward angles hints toward some missing component in the model. In the present work, we do not take into account the interaction of the intermediate off-shell particles which in principle could be quite important. Contribution of coupled channel processes such as the  $pd \rightarrow {}^3\text{He} \pi^0$  may also turn out to be significant. The possibility of other mechanisms, such as the one- and two-body mechanisms taking over at high energies seems unlikely for the following reasons: (i) the momentum transfer in the  $pd \rightarrow {}^3\text{He} \eta$  reaction,

as mentioned in the introduction, continues to be quite large even at high energies (ii) as far as kinematics is concerned, the  $pd \rightarrow {}^3\text{He} \eta$  and  $pd \rightarrow {}^3_\Lambda\text{H} K^+$  reactions are similar. Hence, the results of the theoretical investigation of the  $pd \rightarrow {}^3_\Lambda\text{H} K^+$  reaction up to proton beam energy of 3 GeV [12], where the authors find the one- and two-body mechanisms to contribute 2-3 orders of magnitude lesser than the three-body mechanism at all angles, taken along with similar findings of [2] for  $p\vec{d} \rightarrow {}^3\text{He} \eta$  at  $\theta_\eta = 180^\circ$ , any expectations from the one- and two-body diagrams for  $\eta$  production in reproducing the high energy angular distribution data for the  $pd \rightarrow {}^3\text{He} \eta$  reaction seem remote. Though the effect of the final state interaction has not been studied with the one- and two-body mechanisms, from the present work it seems that at high energies this will only further reduce the cross sections (see Fig. 3 for example), making the one and two-body mechanisms even more negligible.

The above conclusions could probably change if the deuteron and the  ${}^3\text{He}$  have some hitherto unconsidered dynamics (like quarks) at short distances, which influence their structures. Our efforts in future would be to explore such avenues and the role of other possible diagrams such as the direct production of the  $\eta$  meson.

## References

- [1] J. M. Laget and J. F. Lecomte, Phys. Lett. B **194**, 177 (1987).
- [2] J. M. Laget and J. F. Lecomte, Phys. Rev. Lett. **61**, 2069 (1988).
- [3] J. Berger *et al.*, Phys. Rev. Lett. **61**, 919 (1988).
- [4] P. Berthet *et al.*, Nucl. Phys. **A443**, 589 (1985).
- [5] G. Fäldt and C. Wilkin, Nucl. Phys. **A587**, 769 (1995).
- [6] L. A. Kondratyuk and Yu. N. Uzikov, Phys. Atom. Nucl. **60**, 468 (1997);  
nucl-th/9510010;  
L. A. Kondratyuk and Yu. N. Uzikov, Yad. Fiz. **58**, 524, (1995).
- [7] K. P. Khemchandani, N. G. Kelkar and B. K. Jain, Nucl. Phys. **A708**,  
312 (2002).
- [8] B. Mayer *et al.*, Phys. Rev. C **53**, 2068 (1996).

- [9] S. Wycech *et al.*, Phys. Rev. C **52**, 544 (1995);  
G. Fäldt and C. Wilkin, Phys. Rev. C **47**, 938 (1993);  
A. B. Santra and B. K. Jain, Phys. Rev. C **64**, 025201 (2001).
- [10] M. Stenmark, Phys. Rev. C **67**, 034906 (2003).
- [11] R. Bilger *et al.*, Phys. Rev. C **65**, 044608 (2002).
- [12] V. I. Komarov, A. V. Lado and Yu. N. Uzikov, J. Phys. G **21**, L69 (1995); nucl-th/9804050.
- [13] M. Betigeri *et al.*, Phys Lett B **472**, 267, (2000)
- [14] J. Zlomańczuk *et al.*, Acta Phys. Pol. **B33**, 883 (2002).
- [15] R. A. Arndt, I. Strakovsky, R. L. Workman and D. A. Bugg, Phys. Rev. C **48**, 1926 (1993). The amplitudes can be obtained from the SAID program available on internet (<http://gwdac.phys.gwu.edu>).
- [16] M. Batinić *et al.* Phys. Rev. C **51**, 2310 (1995).
- [17] A. Fix and H. Arenhövel, Nucl. Phys. **A697**, 277 (2002).
- [18] R. S. Bhalerao, L. C. Liu, Phys. Rev. Lett. **54**, 865 (1985).